

# Simulation of heat transfer process in absorber channels

Ulugbek Nigmatov<sup>1\*</sup> and Akmaljon Kuchkarov<sup>1</sup>

<sup>1</sup>Fergana Polytechnical Institute, 150107 Fergana, Uzbekistan

**Abstract.** This article describes a mathematical model of heat transfer in absorber channels developed using the «Comsol Multiphysics 5.6. program». The results are presented for determining the longitudinal flow velocity at various sections of the flow channel, heat distribution over time, as well as the heat distribution isoline and isotherm. Developed on the basis of the program «Comsol Multiphysics 5.6.» a simulation model of heat transfer from a photovoltaic battery to a heat absorber can be used to calculate heat and power supply systems. The use of a simulation model in the design of a heat and power supply system makes it possible to reduce the consumption of heat and electricity.

## 1 Introduction

Design of solar power plants, allowing to generate electrical and thermal power on an energetically tangible scale without negative impact on the environment; experimental research and practical application of solar power plants [1-7]; research to improve the efficiency of photoelectric conversion; development and improvement of existing structures for air, water heat supply, cooling and heat removal with forced cooling [8-10]; the widespread use of automated control systems in solar power plants [11-13] are priority areas for the Central Asian region.

A comprehensive study of heat exchange processes makes it possible to reduce the dimensions of heat exchangers in the manufacturing sector by increasing their efficiency.

Actual problems of the theory of heat transfer at present are issues related to the intensification of convective heat transfer. It should be noted here that the problems associated with heat transfer in laminar flow are not widely considered and studied due to the limited number of research works. As is known, according to the theory of the boundary layer, in the laminar regime, the movement of fluid in the near-wall surface transfers heat more efficiently than in the case of flow turbulence. Although a number of developed and researched methods of heat transfer intensification are known, they are classified into two main categories.

There are many recommendations of researchers on the issues of heat transfer in pipes with various types of intensifiers, the constructive solution of which depends on changes in loads, physical properties of the medium, and process features.

---

\* Corresponding author: [ulugbeknigmatov488@gmail.com](mailto:ulugbeknigmatov488@gmail.com)

At present, the issues of systematization of the energy balance, the development of thermal and mathematical models, as well as the generalization of methods and computer programs for calculating photovoltaic thermal modules are relevant.

## 2 Methods

The physical picture of the analyzed flow of a liquid (water) thermal agent and the configuration of the computational domain are [14-15] shown in (Fig. 1, 2). The program “Comsol Multiphysics 5.6.” was used to simulate the process occurring inside the absorber.

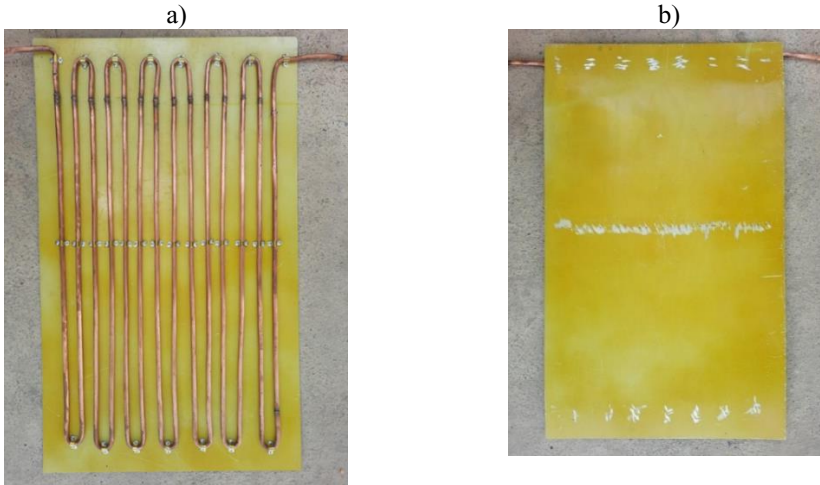


**Fig. 1.** General view of the studied thermal absorber: lower (a) and upper (b) sides.

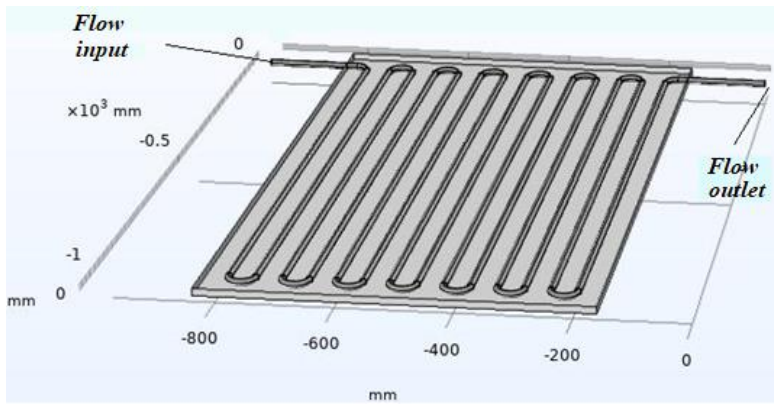


**Fig. 2.** General view of the thermal absorber.

To describe the laminar motion of a liquid (water), a non-stationary system based on the Navier-Stokes equation and the [14] heat distribution equation was used. These equations in cylindrical coordinates  $(z, r, \varepsilon)$  have the following form [15]:

$$\left\{ \begin{aligned} & \frac{\partial r V_z}{\partial z} + \frac{\partial r V_r}{\partial r} + \frac{\partial V_\epsilon}{\partial \epsilon} = 0, \\ & \rho \left( \frac{\partial V_z}{\partial \tau} + V_z \frac{\partial V_z}{\partial z} + V_r \frac{\partial V_z}{\partial r} + \frac{V_\epsilon}{r} \frac{\partial V_z}{\partial \epsilon} \right) = -\frac{\partial p}{\partial x} + \mu \left( \frac{\partial^2 V_z}{\partial z^2} + \frac{\partial^2 V_z}{\partial r^2} + \frac{1}{r^2} \frac{\partial^2 V_z}{\partial \epsilon^2} + \frac{1}{r} \frac{\partial V_z}{\partial r} \right), \\ & \rho \left( \frac{\partial V_r}{\partial \tau} + V_z \frac{\partial V_r}{\partial z} + V_r \frac{\partial V_r}{\partial r} + V_\epsilon \frac{\partial V_r}{\partial \epsilon} - \frac{V_\epsilon^2}{r} \right) = -\frac{\partial p}{\partial r} + \mu \left( \frac{\partial^2 V_r}{\partial z^2} + \frac{\partial^2 V_r}{\partial r^2} + \frac{1}{r^2} \frac{\partial^2 V_r}{\partial \epsilon^2} + \frac{1}{r} \frac{\partial V_r}{\partial r} \right), \\ & \rho \left( \frac{\partial V_\epsilon}{\partial \tau} + V_z \frac{\partial V_\epsilon}{\partial z} + V_r \frac{\partial V_\epsilon}{\partial r} + V_\epsilon \frac{\partial V_\epsilon}{\partial \epsilon} - \frac{V_\epsilon V_r}{r} \right) = -\frac{\partial p}{\partial \epsilon} + \mu \left( \frac{\partial^2 V_\epsilon}{\partial z^2} + \frac{\partial^2 V_\epsilon}{\partial r^2} + \frac{1}{r^2} \frac{\partial^2 V_\epsilon}{\partial \epsilon^2} + \frac{1}{r} \frac{\partial V_\epsilon}{\partial r} \right), \\ & \rho c_p \left( \frac{\partial T}{\partial \tau} + V_z \frac{\partial T}{\partial z} + V_r \frac{\partial T}{\partial r} + \frac{V_\epsilon}{r} \frac{\partial T}{\partial \epsilon} \right) = \frac{\partial}{\partial z} \left( \lambda \frac{\partial T}{\partial z} \right) + \frac{\partial}{\partial r} \left( r \lambda \frac{\partial T}{\partial r} \right) + \frac{1}{r} \frac{\partial}{\partial \epsilon} \left( \lambda \frac{\partial T}{\partial \epsilon} \right). \end{aligned} \right. \quad (1)$$

In the above equations,  $V_z, V_r, V_\epsilon$  are the axial, radial, and tangential components of the flow velocity vector, respectively, and  $T$  is the temperature.  $p$  is the hydrostatic pressure,  $\mu$  is the dynamic coefficient of viscosity,  $c_p$  is the heat capacity,  $\lambda$  is the thermal conductivity.

When dimensionless values are introduced, the pipe diameter,  $D$ , is taken as the length scale, and the average flow rate,  $U_0$  at the pipe inlet, is taken as the velocity scale.

Dimensionless parameters are introduced:

$$U = \frac{V_z}{U_0}, V = \frac{V_r}{U_0}, W = \frac{V_\epsilon}{U_0}, \text{Re} = \frac{\rho D U_0}{\mu}, \text{Pr} = \frac{\lambda}{\mu c_p}.$$

After the introduction of dimensionless quantities, the system equation (1) takes the following form.

$$\left\{ \begin{aligned} & \frac{\partial r U}{\partial z} + \frac{\partial r V}{\partial r} + \frac{\partial W}{\partial \epsilon} = 0, \\ & \frac{\partial U}{\partial \tau} + U \frac{\partial U}{\partial z} + V \frac{\partial U}{\partial r} + \frac{W}{r} \frac{\partial U}{\partial \epsilon} = -\frac{\partial p}{\rho \partial x} + \frac{1}{\text{Re}} \left( \frac{\partial^2 U}{\partial z^2} + \frac{\partial^2 U}{\partial r^2} + \frac{1}{r^2} \frac{\partial^2 U}{\partial \epsilon^2} + \frac{1}{r} \frac{\partial U}{\partial r} \right), \\ & \frac{\partial V}{\partial \tau} + U \frac{\partial V}{\partial z} + V \frac{\partial V}{\partial r} + W \frac{\partial V}{\partial \epsilon} - \frac{W^2}{r} = -\frac{\partial p}{\rho \partial r} + \frac{1}{\text{Re}} \left( \frac{\partial^2 V}{\partial z^2} + \frac{\partial^2 V}{\partial r^2} + \frac{1}{r^2} \frac{\partial^2 V}{\partial \epsilon^2} + \frac{1}{r} \frac{\partial V}{\partial r} \right), \\ & \frac{\partial W}{\partial \tau} + U \frac{\partial W}{\partial z} + V \frac{\partial W}{\partial r} + W \frac{\partial W}{\partial \epsilon} - \frac{WV}{r} = -\frac{\partial p}{\rho \partial \epsilon} + \frac{1}{\text{Re}} \left( \frac{\partial^2 W}{\partial z^2} + \frac{\partial^2 W}{\partial r^2} + \frac{1}{r^2} \frac{\partial^2 W}{\partial \epsilon^2} + \frac{1}{r} \frac{\partial W}{\partial r} \right), \\ & \frac{\partial T}{\partial \tau} + U \frac{\partial T}{\partial z} + V \frac{\partial T}{\partial r} + \frac{W}{r} \frac{\partial T}{\partial \epsilon} = \frac{1}{\text{Re Pr}} \frac{\partial}{\partial z} \left( \frac{\partial T}{\partial z} \right) + \frac{1}{\text{Re Pr}} \frac{\partial}{\partial r} \left( r \frac{\partial T}{\partial r} \right) + \frac{1}{\text{Re Pr}} \frac{1}{r} \frac{\partial}{\partial \epsilon} \left( \lambda \frac{\partial T}{\partial \epsilon} \right). \end{aligned} \right. \quad (2)$$

Obvious no-slip boundary conditions are set on all fixed solid walls  $U|_{hb} = 0, V|_{hb} = 0$  and  $W|_{hb} = 0$ , where  $hb$  – hard border. At the channel outlet in the section for horizontal and vertical velocities, the standard extrapolation conditions are accepted.

$$\frac{\partial^2 U}{\partial z^2} = \frac{\partial^2 V}{\partial z^2} = \frac{\partial^2 W}{\partial z^2} = 0.$$

*Numerical scheme.* The dimensionless Navier-Stokes equation in vector form will have the following form:

$$\frac{\partial F}{\partial t} + U \frac{\partial F}{\partial x} + V \frac{\partial F}{\partial y} = \frac{\partial}{\partial z} \left( A \frac{\partial F}{\partial z} \right) + \frac{\partial}{r \partial r} \left( A \frac{\partial F}{\partial r} \right) + \frac{\partial}{r^2 \partial \varepsilon} \left( A \frac{\partial F}{\partial \varepsilon} \right) + P^F. \quad (3)$$

Here:  $x$

*McCormack's scheme.* As is known, the McCormack method [16-18] is widely used to solve the equations of gas dynamics. McCormack's method is especially useful for solving non-linear partial differential equations.

Applying the explicit «predictor-corrector» method to the nonlinear Navier-Stokes equation, we obtain the following difference scheme:

**Predictor:**

$$\begin{aligned} \bar{F}_{i,j,k} = & F_{i,j,k}^n - \Delta t \left( U_{i,j,k}^n \frac{F_{i+1,j,k}^n - F_{i,j,k}^n}{\Delta z} + V_{i,j,k}^n \frac{F_{i,j+1,k}^n - F_{i,j,k}^n}{\Delta r} + W_{i,j,k}^n \frac{F_{i,j,k+1}^n - F_{i,j,k}^n}{\Delta \varepsilon} \right) + \\ & + \Delta t \left( \frac{\bar{F}_{i,j+1,k}^n - 2F_{i,j,k}^n + F_{i,j-1,k}^n}{Re \Delta r^2} + \frac{F_{i+1,j,k}^n - 2F_{i,j,k}^n + F_{i-1,j,k}^n}{Re \Delta z^2} + \frac{F_{i,j,k+1}^n - 2F_{i,j,k}^n + F_{i,j,k-1}^n}{Re \Delta \varepsilon^2} + P^F \right). \end{aligned} \quad (4)$$

**Corrector:**

$$\begin{aligned} & F_{i,j,k}^{n+1} = \\ & \frac{1}{2} \left( \bar{F}_{i,j,k} + F_{i,j,k}^n - \Delta t \left( U_{i,j,k}^n \frac{F_{i,j,k}^n - F_{i-1,j,k}^n}{\Delta z} + V_{i,j,k}^n \frac{F_{i,j,k}^n - F_{i,j-1,k}^n}{\Delta r} + W_{i,j,k}^n \frac{F_{i,j,k}^n - F_{i,j,k-1}^n}{\Delta \varepsilon} \right) + \right. \\ & \left. + \Delta t \left( \frac{\bar{F}_{i,j+1,k}^n - 2\bar{F}_{i,j,k}^n + \bar{F}_{i,j-1,k}^n}{Re \Delta r^2} + \frac{\bar{F}_{i+1,j,k}^n - 2\bar{F}_{i,j,k}^n + \bar{F}_{i-1,j,k}^n}{Re \Delta z^2} + \frac{\bar{F}_{i,j,k+1}^n - 2\bar{F}_{i,j,k}^n + \bar{F}_{i,j,k-1}^n}{Re \Delta \varepsilon^2} + P^F \right) \right). \end{aligned} \quad (5)$$

This explicit scheme of the second order of accuracy with the approximation error  $O\left((\Delta t)^2, (\Delta z)^2, (\Delta r)^2, (\Delta \varepsilon)^2\right)$  is stable for  $U_{\max} \Delta t \left( \frac{1}{\Delta z} + \frac{1}{\Delta r} + \frac{1}{\Delta \varepsilon} \right) < 1$ , which corresponds to the Courant conditions [12].

Initially, the (predictor) is found with the  $F_i^{n+1}$  value and at the  $n + 1$ -th time step, and then the (corrector) is determined by the final value of  $F_i^{n+1}$  at the  $n + 1$ -th time step. Note that the predictor is approximated by forward differences, and the corrector is approximated backward by differences.

A similar scheme was used for transverse speed. A feature of discretization is that the finite difference approximation is centered according to the chosen pattern. In this case, the grid indices for the dependent variables turn out to be shifted.

The velocities obtained according to schemes (5) do not satisfy the continuity equation. Therefore, following the SIMPLE procedure [19-21], we introduce a pressure correction  $\delta p_{i,j}$  that satisfies the condition

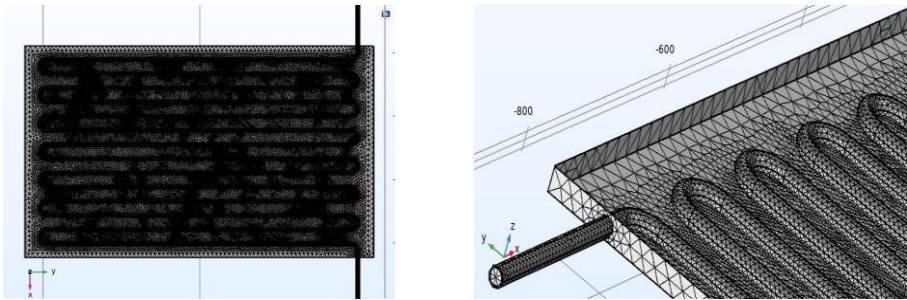
$$\left\{ U_{i,j}^{n+1} = U_{i,j}^n - \Delta t \frac{\partial \delta p_{i,j}}{\partial x}, V_{i,j}^{n+1} = V_{i,j}^n - \Delta t \frac{\partial \delta p_{i,j}}{\partial y} \right. \quad (6)$$

Now, substituting the velocities  $\tilde{U}_{i,j}^{n+1}$ ,  $\tilde{V}_{i,j}^{n+1}$  into the continuity equation, it is easy to obtain the following equation

$$\left(\frac{\delta p_{i+1,j} - 2\delta p_{i,j} + \delta p_{i-1,j}}{\Delta x^2}\right) + \left(\frac{\delta p_{i,j+1} - 2\delta p_{i,j} + \delta p_{i,j-1}}{\Delta y^2}\right) = \frac{1}{\Delta t} \left(\frac{U_{i+1,j}^{n+1} - U_{i-1,j}^{n+1}}{2\Delta x} + \frac{V_{i,j+1}^{n+1} - V_{i,j-1}^{n+1}}{2\Delta y}\right). \tag{7}$$

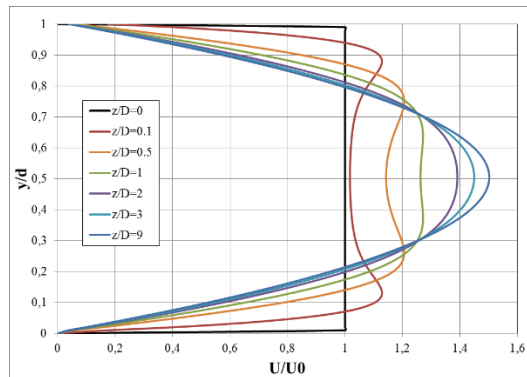
To solve equation (7), we used the iterative method of upper relaxation. Thus, according to (5), intermediate values of the parameters are determined, then, according to equation (7), the correction pressure is determined. Therefore, the pressure on time layer  $n + 1$  will be equal to  $p^{n+1} = p^n + \delta p$ .

Figure 3 shows a difference grid in which 973128 cells are used.



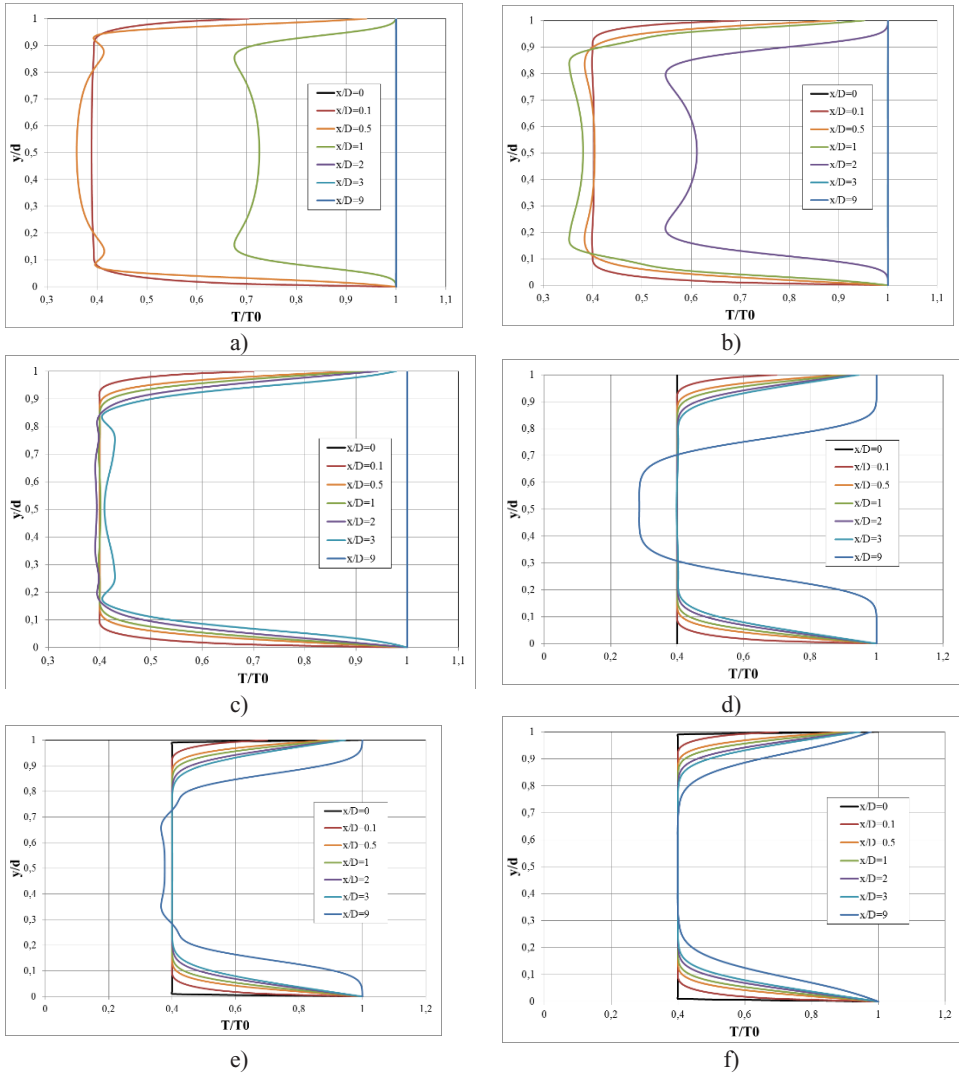
**Fig. 3.** General view of the difference grid.

Figure 4 shows the results of determining the longitudinal flow velocity at various sections of the flow channel, with the Reynolds number  $Re = 500$ .



**Fig. 4.** The results of determining the longitudinal flow velocity at various sections of the flow channel.

It can be seen from (Fig. 4) that the flow in sections  $z / D = 9$  has a laminar profile. (Fig. 5) shows the results of heat distribution when the valve is opened at different times.



**Fig. 5.** The results of heat distribution over time: a)  $T = 1$  s; b)  $T = 2$  s; c)  $T = 5$  s; d)  $T = 8$  s; e)  $T = 10$  s; f)  $T = 15$  s.

Figure 6 shows the heat distribution isoline and isotherm.

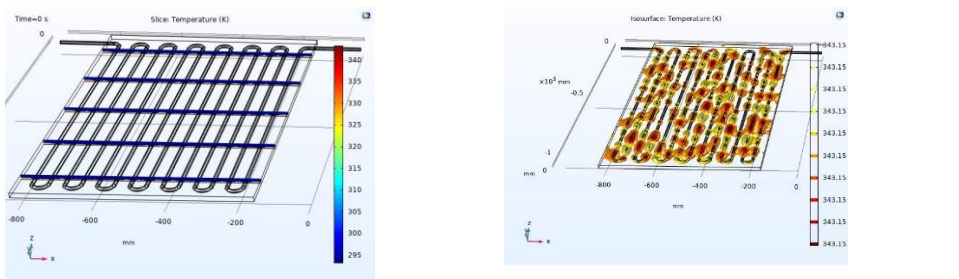


**Fig. 6.** Isolines of heat distribution and isotherms.

### 3 Conclusion

In engineering practice, when calculating the heat and power indicators of thermal absorbers, the use of the Comsol Multiphysics 5.6. allows you to speed up the process of calculating their heat transfer and hydrodynamics, to create a difference grid for introducing initial and boundary conditions for the calculation. The number of cells in the difference grids depends on the tolerances provided by the standards for the calculation of heat exchange processes. Depending on the Reynolds number and the diameter of the channel of the thermal absorber, it is possible to determine the stabilization section, the laminar flow section, as well as the fluid velocity and heat transfer, respectively.

Developed on the basis of the program "Comsol Multiphysics 5.6." a simulation model of heat transfer from a photovoltaic battery to a heat absorber can be used to calculate heat and power supply systems.

The use of a simulation model in the design of heat and power supply systems makes it possible to reduce the consumption of heat and electricity.

### References

1. Ergashev, S.F. Applied Solar Energy (English translation of Geliotekhnika), 2006, **42(4)**, 29–31.
2. Ergashev, S.F., Kuldashov, O.K. & Mamasodikova, U.Y. Appl. Sol. Energy **43**, 68–71 (2007). <https://doi.org/10.3103/S0003701X07020028>
3. Kokhova, I.I., Kabakov, V.I., Ergashev, S.F., Drobyazgina, O.S. Geliotekhnika, 1991, **2**, 14–16.
4. Uktam Salomov, Akmal Kuchkarov, Omad Urishev and Olmosbek Mamatov. BIO Web of Conferences **84**, 05029 (2024). <https://doi.org/10.1051/bioconf/20248405029>
5. Muxammade Sultanxan Payzullaxanov, Uktam Salomov, Akmal Kuchkarov, Olmosbek Mamatov and Abdurashid Xolmatov. BIO Web of Conferences **84**, 05030 (2024), <https://doi.org/10.1051/bioconf/20248405030>
6. Kuchkarov, A. A., Abdumuminov, A. A., & Abdurakhmanov, A. (2020). Applied Solar Energy **56**, 192-197.
7. Akbarov, R. Y., & Kuchkarov, A. A. (2018). Applied Solar Energy **54**, 183-188.
8. Klychev, S. I., Abdurakhmanov, A. A., & Kuchkarov, A. A. (2014). Applied Solar Energy **50**, 168-170.
9. Abdurakhmanov, A., Kuchkarov, A. A., Mamatkosimov, M. A., Sobirov, Y. B., & Akhadov, J. Z. (2016). Applied Solar Energy **52(2)**, 137.
10. Abdurakhmanov, A., Kuchkarov, A. A., Mamatkosimov, M. A., & Sobirov, Y. B. (2015). Applied Solar Energy, **51**, 301-305.
11. Kuchkarov, A. A., Sobirov, Y. B., Mamatkasimov, M. A., Abdumuminov, A. A., & Abdurakhmanov, A. A. (2016). Applied Solar Energy, **52**, 215-219.
12. Akhadov, Z. Z., Abdurakhmanov, A. A., Sobirov, Y. B., Kholov, S. R., Mamatkosimov, M. A., & Kuchkarov, A. A. (2014). Applied Solar Energy **50(2)**, 122.
13. Orlov S. A., Klychev S. I. Applied Solar Energy. **54**, 61-64 (2018)
14. Loitsyansky L. G. The mechanics of fluid and gas. (Moscow, Science, 1987).
15. Kuchkarov, A. A., Muminov, S. A., & Madaliyev, M. E. (2023). Applied Solar Energy, **59(5)**, 665-671.

16. Robert S. Bernard, *Computers & Mathematics with Applications*, **24(5–6)**, 1992, 151-168, ISSN 0898-1221, [https://doi.org/10.1016/0898-1221\(92\)90046-K](https://doi.org/10.1016/0898-1221(92)90046-K).
17. Jim Douglas Jr., *Quart. Appl. Math.* **14** (1956), 333–335. MR 88805. DOI <https://doi.org/10.1090/S0033-569X-1956-88805-1>
18. Patankar, S.V. (1980). *Numerical Heat Transfer and Fluid Flow* (1st ed.). CRC Press, P. 200. <https://doi.org/10.1201/9781482234213>
19. Abdukarimov, B., Kuchkarov, A., Botirov, D., & Nazirjonova, S. (2024). *BIO Web of Conferences* **84**, 05033. EDP Sciences.
20. Ismailov, B., Babakhodzhaev, R., Kuchkarov, A., Mamatov, O., Ismailov, K., Hamdamov, D., & Qipchaqova, G. (2024). *BIO Web of Conferences* **84**, 02023 EDP Sciences.
21. Akmal Kuchkarov, Shermuhammad Muminov and Semen Frid et al. *BIO Web of Conferences*. **84**, 01041 (2024) DOI: 10.1051/bioconf/20248401041